Charge Storage on Ionic Liquid Electric Double Layer: The Role of the Electrode Material

ARTICLE *in* ELECTROCHIMICA ACTA · FEBRUARY 2015

Impact Factor: 4.5 · DOI: 10.1016/j.electacta.2015.02.180

1 AUTHOR:

Renata Costa
University of Porto
12 PUBLICATIONS **186** CITATIONS

SEE PROFILE

Electrochimica Acta 167 (2015) 421–428

Contents lists available at ScienceDirect

Electrochimica Acta

journal homepage: www.elsevier.com/locate/electacta

Charge Storage on Ionic Liquid Electric Double Layer: The Role of the Electrode Material

Renata Costa, Carlos M. Pereira *, A. Fernando Silva *

Faculdade de Ciências da Universidade do Porto, Departamento de Química e Bioquímica, CIQUP-Physical Analytical Chemistry and Electrochemistry Group, Rua do Campo Alegre, s/n 4169 – 007 Porto, Portugal

ARTICLE INFO

Article history:
Received 9 February 2015
Accepted 20 February 2015
Available online 20 March 2015

ABSTRACT

The influence of the electrode surface material, the ions chemical structure and the combination of both on differential capacitance curves plays an important role to a deeper understanding on the molecular level structure of electrical double layers (EDLs) involving ionic liquids (ILs).

The research work focused on the structure of ionic liquids on charged surfaces is technologically-important for the development of new applications and in the upward of the existing ones, such electrodeposition or energy storage and conversion. Understanding EDL property will allow maximizing the specific capacitance, which in turn leads to higher energy and powering densities of the devices. The electronic interactions of 1-butyl-3-methylimidazolium (tris(pentafluoroethyl)trifluorophosphate) [C_4MIM][FAP] ionic liquid with Hg, Au, Pt and GC were assessed in order to get a fundamental understanding of the electrical double layer microscopic structure and its intrinsic properties at electrode/IL interface. Ionic liquids containing the $[FAP]^-$ anion exhibit a strong hydrophobic nature and wider electrochemical window than previously used ionic liquids and a good electrochemical stability. The magnitude and shape of C(E) curves revealed different orientations of the cation when the nature of the substrate is changed. The predominantly hydrophobic interactions of the imidazolium hydrocarbon chains with the Hg are traduced by the camel shape type curve. In contrast, the low and nearly constant C (E) values obtained for Au electrode point to the interfacial structure being dominated by the electrostatic π-stacking of the imidazolium ring/electrode interaction with the aromatic ring adopting an orientation more parallel to the surface.

1. Introduction

The bulk molecular structure of ionic liquids outcomes from a delicate balance between the long-range forces (Coulombic) and short-range forces (van der Waals, dipole-dipole, hydrogen bonding). The ion-ion interactions of ILs provide a fundamental understanding of the electronic structure and specific interactions that occur within the ionic liquid. The extent and strength of the intermolecular interactions between anions and cations (such coulombic and hydrogen bonding interactions) are usually invoked to explain the physical properties and reaction dynamics of these Coulombic fluids [1].

Despite the behavior of room temperature ionic liquids (RTILs) near charged surfaces is receiving increasing attention, there is still some controversy and lack of consensus in understanding how the pure ionic liquid is structured at charged and uncharged surfaces.

At electrified surfaces, the above mentioned interactions are additionally modulated by the applied potential.

Over recent years, the study of anion-cation interactions [2,3], nanostructural organization [4–7] and different conformations of anions [8] and cations [9] in both liquid phase and in the crystalline structure, have been the subject of considerable interest. Evidence of micro and nano heterogeneities emerged from theoretical studies involving molecular dynamics simulations performed by Wang et al. [10] and Pádua et al. [4] concerning the nanostructural organization were corroborated by Triolo et al. [11] and Bodo et al. [12] through X-ray measurements. The structural heterogeneity resulting from the aggregation of the alkyl side chains of the nonpolar substituent imidazolium cations plays an important role in the properties of the liquid making them distinguishable from the molecular solvents. The absence of solvent molecules in the molten salts with high melting temperatures and ionic liquids

* Corresponding author. Tel.: +351 22040613; fax: +351 220402659.
E-mail addresses: cmpereir@fc.up.pt (C.M. Pereira), afssilva@fc.up.pt (A. F. Silva).

http://dx.doi.org/10.1016/j.electacta.2015.02.180
0013-4686/

raises the challenge to develop models capable to describe the structural properties of interfaces constituted only by ions.

The IL/electrode interfacial structure models proposed until now range from the Helmholtz double layer and a multilayered structure, with the ions exhibiting a pronounced oscillatory structure close to the interface. Extensive work concerning simulation techniques was done to better comprehend the electrode–electrolyte interfaces, enlightening that the ions adopt a multilayered structure at the ionic liquid/graphite (planar) electrode interface. Kislenko et al. [13] performed molecular dynamics simulation in order to evaluate the structure of the electrical double layer in the ionic liquid l-butyl-3-methylimidazolium hexafluorophosphate ([C_4MIM][PF_6]) near a basal plane of graphite. It was found that near an uncharged surface the IL structure differs from its bulk structure exhibiting a well-ordered region. At the negatively charged graphene sheet was found to be composed by alternated cationic and anionic layers.

Increasing efforts have been made in the past few years to investigate the interfacial region at electrode/IL systems; however, information of ILs in contact with charged surfaces is still scarce. Considering the significant experimental and computer simulations progress in the study of electrode/ionic liquid interface, the EDL models proposed so far do not appropriately accommodate the influence of the chemical nature of ionic liquids and their interactions with the surface.

Ionic liquids containing the tris(pentafluoroethyl)trifluorophosphate $[FAP]^-$ anion paired with imidazolium, pyrrolidinium and phosphonium cations exhibit a strong hydrophobic nature and wider electrochemical windows than $[PF_6]^-$ or equivalent ionic liquids [14], making them ideal candidates as extraction solvents [15] and energy storage devices electrolytes [16].

Since the interfacial effects of ionic liquids at charged surfaces are very relevant for electrochemical applications of ionic liquids, following the ion arrangement at the interface is fundamental in order to give a comprehensive understanding of how nanostructuration observed in the bulk will affect the EDL structure.

The high-energy X-ray reflectivity results obtained by Mezger et al. [17] considering ionic liquids with $[FAP]^-$ anions in contact with charged sapphire substrate point to an interfacial molecular layering structure. AFM studies have shown that the molecular structure and, consequently, the interfacial properties of ionic liquids at charged surfaces can be modulated not only by changing the surface potential, but also by varying chemical composition of the ionic liquids [18]. From AFM results obtained with pyrrolidinium and imidazolium $[FAP]^-$ ILs at Au(111) surface, it was possible to conclude that ILs are strongly adsorbed onto solid surfaces with several IL layers presenting oscillating ion density profiles at the electrode surface [19].

The multilayer type model is the most common accepted model to describe the IL/electrode structure, however some authors advance another possible arrangement of the ions at the interface such as the monolayer type structure [20]. Baldelli's description of the charge arrangement of the cation and anion at the interface resembles the classical Helmholtz picture of an ionic monolayer at a charged surface, e.g., ionic liquids are organized into one ion layer thick [20].

To accomplish a better understanding of charged solid-electrolyte interfaces, a systematic study was followed in order to discriminate the contribution of the ion-ion and ion-electrode material interactions on the electrochemical performance of systems containing $[FAP]^-$ ionic liquids. The novelty of this work is based upon the proposal of an interfacial structure for each electrode studied based on the shape of the differential capacity curves.

2. Experimental

2.1. Reagents

The hydrophobic ionic liquid [C_4MIM][FAP] was purchased to Merck with the highest purity grade available (higher than 99%).

The IL purification procedure included the washing of the ionic liquid several times consecutively using ultra-pure water with continuous stirring in order to dissolve and remove water soluble impurities. To reduce the water content to the lowest minimum, before electrochemical study, the IL was heated for several hours at $80 \pm 5\,^{\circ}C$ under vacuum and ($\approx$10 Pa) with stirring. The water content, according to Karl-Fisher titration (831 KF coulometer Metrohm) was below 30 ppm.

Before each experiment all glass material was washed with concentrated sulfuric acid followed by abundant washing with ultra pure water and finally with boiling ultra-pure water. The ultra-pure water was obtained by filtration through Milli-Q deionized water purification system with a volume resistivity of not less than 18.2 MΩ cm.

The experiments were performed in a three electrode electrochemical cell assembled. Mercury electrode (Metrohm 663 VA Stand), Au, Pt or GC were used as working electrode. Autolab 302 N potentiostat EcoChemie equipped with a frequency analyzer (FRA) was used in the electrochemical studies. The cell is surrounded by a glass jacket allowing water circulation to keep the temperature of the system at a required value. A silver wire was used as pseudo-reference electrode and glassy carbon was used as auxiliary electrode. The IL was purged with pure Nitrogen to remove dissolved oxygen for at least 30 min. During the experiments, N_2 was kept over the electrolyte without disturbing the electrochemical measurements.

As mentioned in the literature, an important factor in the use of solid electrodes is the dependence of the electrode response (in terms of activity, stability and reproducibility) relatively to the surface conditions. Consequently, the surface requires a specific pre-treatment in order to obtain reproducible results. The characteristic voltammogram obtained indicates the perfectness of solid surfaces, cleanliness of the cell used and quality of the reference electrode.

The polycrystalline Au, Pt and CG used in the characterization of ionic liquids were acquired to Metrohm (0.0314 cm^2) and consist in a polished hard disk imbebed PEEK cylinder. Before each study, the electrodes were polished with 1 micron diamond paste (Buehler) during 2 minutes and washed with abundant ultra-pure water to remove any diamond paste trace remaining in the electrode surface. Subsequently, the Au electrode treatment proceeded with electrochemical cleaning in a perchloric acid solution (Aldrich, 70%) with concentration of 0.1 M until a stable electrochemical profile is reached. For Pt electrode the surface was electrochemically cleaned in 0.5 M H_2SO_4 aqueous solution. The first step of cleaning consisted in holding the Pt electrode at +2.0 V *vs.* SCE for 2 min in order to anodically dissolve any organic trace residues. The following step consisted in cycling the electrode between -0.23 and +1.10 V *vs.* SCE at 100 mV/s, stopping after 10-20 cycles at the positive limit (+1.10 V) *vs.* SCE. The voltammetric profiles of the Pt electrode were in good agreement with the previously reported voltammograms [21].

The electrocapillary curve was obtained by measuring the lifetime of a set of 10 Hg drops falling at a constant potential within the ideal polarizability window estimated by cyclic voltammetry measuring the time at which the drop falls. The applicability of the technique to determine the pzc and the extraction of the capacitance values is described in our previous work [22,23].

The size of the ions was estimated using ChemBio3D Ultra 13.0 modeling program (Perkin Elmer).

3. Results

One of the most important properties of ILs relevant to electrochemistry is their wide electrochemical potential windows (EW). Indeed, the electrochemical potential window is a potential range between which the electrolyte or the electrode material is not oxidized or reduced. The EW characterizes the electrochemical stability of ionic liquids, i.e., the limits of the window which correspond to the start of the electrochemical decomposition of the involved ions/or electrode material.

Within the electrochemical window, potential dependent adsorption/desorption processes of the ions and the role of the electrode material have been monitored by cyclic voltammetry and are showed in Fig. 1.

Since the electrochemical potential window is sensitive to impurities, by analyzing Fig. 1 it is clear that the CVs did not show any evidence of the presence of impurities within the potential range considered.

The Hg electrode was the electrode material that allowed assessing more negative potentials. The widest electrochemical window was obtained at the GC substrate with 3.6 V *vs.* Ag taking into account a current cut-off of 10 $\mu A\,cm^{-2}$.

The cathodic electrochemical stability increase in order Au<Pt<GC<Hg and the anodic limit increase Hg<GC≈Pt≈Au. The AC EWs performed by Yang et al. [24] on different electrode materials followed the same trend found in this work, i. e., EWs Au<Pt<GC and were found to be consistent with the tendency measured in the DC electrochemical stability of [C_4MIM][BF_4] IL.

A clear dependence of the anodic stability on the anion was observed by Weingarth et al. [25] with cyclic voltammetry and confirmed by XPS valence band spectra for ionic liquid systems containing cyano groups in the anion.

The work carried out by Lo et al. [26] at Pt/1-butyl-1-methylpyrrolidinium salicylate ionic liquid present experimental and theoretical proofs that confirm that the cathodic limit is determined by the reduction of the anion rather than the reduction of cation.

Menshykau et al. [27] evaluated the influence of electrode roughness on cyclic voltammetry. The authors found that the electrode roughness only has a markedly effect on the shape of cyclic voltammograms and peak currents at extremely high values of electrode roughness. The authors also found that a different degree of polishing on glassy carbon surface does not give observable effects in cyclic voltammetry experiments.

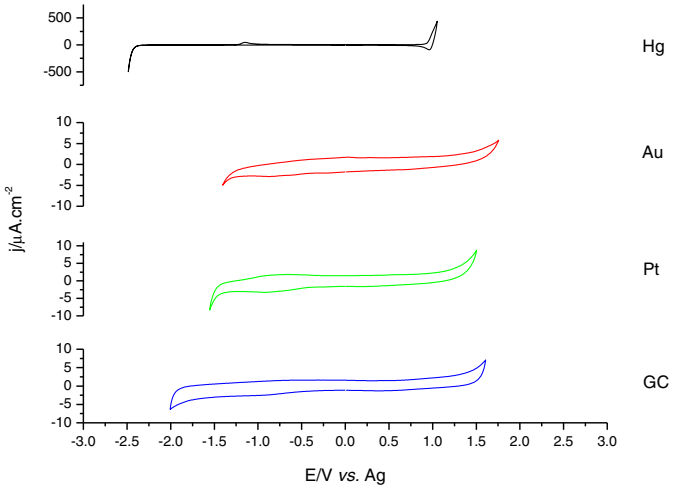

Fig. 1. Cyclic voltammograms measured at [C_4MIM][FAP]/Hg, Au, Pt and GC interfaces.

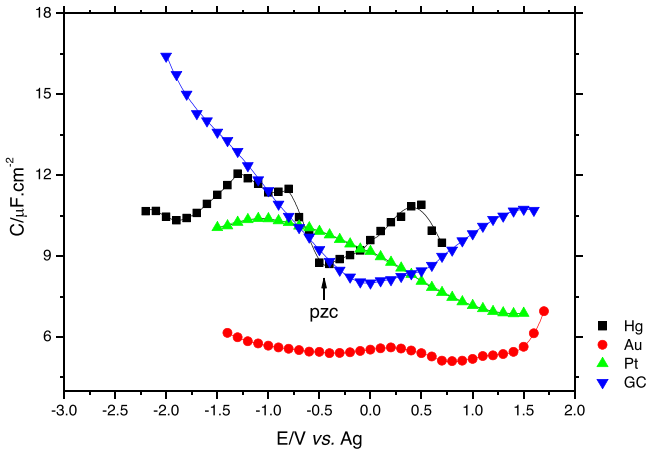

Fig. 2. C(E) curves measured at [C_4MIM][FAP]/Hg, Au, Pt and GC interfaces.

The potential dependent electric double layer structure of [C_4MIM][FAP] ionic liquid at different electrode materials was assessed by impedance data and the C(E) curves measured at Hg, polycrystalline Au and Pt and at non-metallic GC electrode are displayed in Fig. 2.

From the analysis of Fig. 2 there is no doubt that the nature of the electrode material, e.g. the interaction ion-electrode, is crucial in defining the overall shape of C(E) curves. The relation between C (E) curves with EDL structure is the starting point to many EDL models, revealing that the shape of differential capacitance versus electrode potential can change quantitative and qualitatively with the structure of the electrode surface. The trend here reported is in contrast with the C(E) curves presented by Lockett et al. [28] for 1-butyl-3-methylimidazolium [C_4MIM][PF_6] which were insensitive to the nature of electrode surface. In our previous work [22], we have obtained the differential capacitance–potential curves of [C_4MIM][PF_6] in contact with Hg, Pt and GC electrodes by fitting electrochemical impedance spectra to an R-CPE equivalent circuit. The C(E) curves were found to vary with the applied potential and the shape was sensitive to the electrode nature with C_{min} following the order Hg > GC > Pt.

The influence of the electrode material on the differential capacity was suggested in 1964 by Frumkin et al. [22] and later highlighted by Trasatti et al. [29]. Main influences come from the chemical nature, structure and physical state of the surface, in particular the preparation processes of these surfaces. Trasatti characterized the perturbation on surface potentials of each phases consequently due to the presence of the adjacent phase by establishing the relationship between the specific adsorption and pzc, which depend on the nature of the electrode, essentially centered on a property referred as “extraction work” (φ).

In this study, the topography of the electrode surface change qualitatively the C(E) shapes and simultaneously seems to affect the adsorption characteristics of the ionic layer adjacent to the electrode. The C(E) curves vary from camel-shape (Hg), flat bell shape with a local maximum (hump) at +0.13 V *vs.* Ag (Au), asymmetric bell shape for Pt electrode and U shape for GC substrate (Fig. 2).

Nevertheless, the reason why C(E) curves shows different dependence as function of the applied potential for different electrode/electrolyte systems remains unclear. The differential capacity as a function of applied potential is determined by the distribution of charge in the first adjacent layers in contact with the electrode, so this property should be very sensitive to conformational changes of the cations and anions located in these layers. Alam et al. [30] also assessed the role of the electrode material by measuring C(E) curves at Hg, GC and

Au/1-propyl-3-methylimidazolium tetrafluoroborate ionic liquid interfaces which were found to be highly sensitive to the substrate nature.

3.1. Hg

The C(E) curve measured at smooth mercury surface show a slightly asymmetric camel-shape curve with a minimum close to the pzc flanked by two maxima peaks with decreasing wings at larger positive and negative electrode potentials.

The Hg surface is energetically uniform and easily renewable presenting peculiar characteristics of repeatability and reproducibility. We took the advantage of using the mercury electrode for the direct determination and further correlation of the experimental pzc with the maximum or minimum of the C(E) curve providing the possibility to check the theoretical predictions on the structure of the electrical double layer in ionic liquids. The value of pzc obtained from the maximum of the drop time curve was -0.45 ± 0.03 V. It is worth to underline that at the pzc the electrostatic interaction between ions and electrode surface is defined as zero which gives fundamental information in surface science. The pzc determined for [C_4MIM][FAP] coincide with the differential capacitance minimum which is in contrast to what was obtained at Hg/[C_4MIM][PF_6] (pzc does not coincide with the potential of the differential capacitance minimum) [22]. Nanjundiah et al. [31] measured differential capacity curves of dropping mercury electrodes in contact with a series of ionic liquids comprising the same cation (1-ethyl-3-methyl imidazolium) and different anions $[CF_3SO_2]_3C^-$, $[CF_3SO_2]_3N^-$, $CF_3SO_2^-$ and BF_4^-. The authors found that the pzc do not coincide with the minimum of differential capacitance curves.

Since ILs can be composed with different ion pairs, the ion size seems to affect the EDL structure and differential capacitance. Corroborated by theoretical studies [32], the experimental results seems to point by increasing the symmetry of the cation *vs.* anion shifts the pzc towards more negative potentials and promotes the appearance of a minimum coincident with the pzc in C(E) curve [33]. This observation may be due to the overscreening effects dominating near the potential at the point of zero charge which is enhanced by larger anions.

The accordance between simulations and electrochemical experiments remains qualitative and a though task. Using a mean-field model a camel-shaped capacitance curve was predicted by Kornyshev [34] when the excluded volume and the "compressibility" of the double layer is considered. The camel shape profile was also predicted by Fedorov et al. [35] and by Georgi et al. [36] based on a model considering spherical and elongated ions with charged 'parts' and neutral 'tails. A double-hump camel shaped C(E) curve was reported if one of the ions in the IL present neutral moieties. Studies carried out by Fedorov and Kornyshev [32] by means of molecular dynamics simulations for a dense set of Lennard-Jones spheres between charged interfaces also predicted that the asymmetry on differential capacity can occur if the differences in the size of the anions and cations are considered. Even the charge distribution inside a given ion should be considered.

Trulsson et al. [37] found by coarse-grained model and Monte Carlo simulations that the depth of the minimum observed on the camel-shaped C(E) curve near the potential of zero charge was also considerably affected by the ion–surface dispersion interactions. MD simulations carried out by Trulsson et al. [37] also highlighted that the presence of dispersion forces play an important role at interfaces and the camel shape profile is a result from the decrease of the van der Waals forces among the ionic species near the electrode.

Asymmetric "camel shape" curves can also be obtained for ionic liquids composed of ions of equal size, however, with different specific affinity for the electrode surface. Lauw et al. [38] examined the EDL at the IL/electrode interface with a numerical self-consistent mean-field theory and found that polarizability effects, modeled including an effective dielectric constant can also promote camel-shaped C(E) curves.

Atomistic MD simulations performed by Vatamanu et al. [39] also obtained the camel-shaped curve in a system of a pyrrolidinium ionic liquid at graphite electrodes interface.

These theoretical predictions coupled to our experimental results enlighten the importance that shape anisotropy and charge distribution of ions play in shaping the EDL.

Considering the hydrophobic nature of Hg electrode it is expected that the imidazolium cation interacts with the surface via their aliphatic alkyl side chains at larger negative potentials. As the potential is made less negative, the interface become more populated by the $[FAP]^-$ occurring an expected loss in surface enrichment of the imidazolium aliphatic alkyl chains. The presence of the charged surface leads to a strong organization of the ionic region near the electrode surface resulting in a multilayer structure formed by interpenetrated polar and non polar domains modulated by the applied potential.

A X-ray reflectometry study was carried out in order to clarify the external electric field dependence of an IL-EDL structure and it was found that an increasing degree of ordering of the layering structure is achieved by controlling the magnitude of the applied voltage [40].

In order to better rationalize the possible orientation that the ions can adopt at the mercury charged surface, the charge density curve was obtained from the integration of the differential capacity curve (Fig. 3).

By analyzing Fig. 3 it is clear that the absolute value of charge at negative rational potentials grows with greater intensity than at positive rational potentials, possibly reflecting the higher adsorbability of the cation compared with the anion. The σ(E) curve present two linear branches at $\sigma << 0$ and at $\sigma >> 0$. As in our previous work, by assuming a simple Helmholtz type layer model at extreme polarizations, the thickness of the double layer can be estimated by using Eq. (3) [32].

$$d = \frac{\varepsilon_0 \varepsilon}{K} \tag{3}$$

where ε is the relative permittivity, ε_0 is permittivity of the vacuum (in $\mu F\,m^{-2}$) and K the limiting slope of the σ(E) curve. The thickness of the double layer was estimated using the value of 8 as relative permittivity [33]. The general arguments

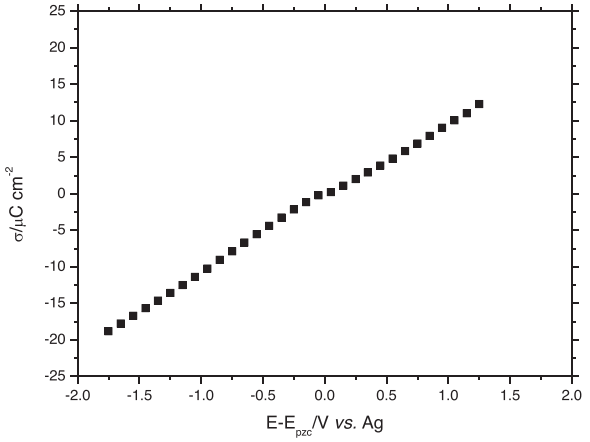

Fig. 3. Charge density curve measured at Hg/[C_4MIM][FAP] interface at 20 °C.

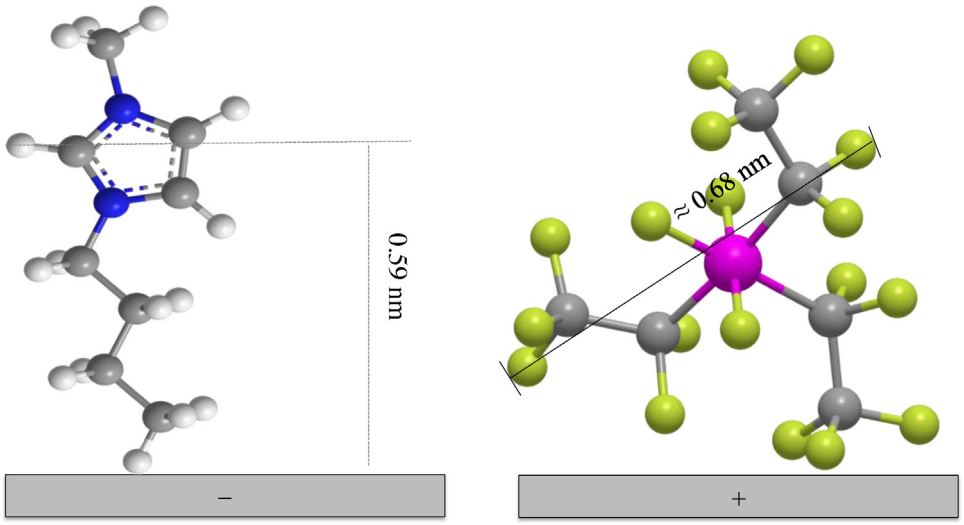

Scheme 1. Estimated sizes of $[C_4MIM]^+$ cation and $[FAP]^-$ anion using ChemDraw13 software.

about the choice of this method were discussed in our previous work [41].

For $\sigma << 0$ the values of d estimated is approximately 0.63 nm which is in excellent accordance with the estimated value for the liquid containing the same cation $[C_4MIM]^+$ using a $[Tf_2N]^-$ anion (bis(trifluoromethylesulfonyl) imide) as counter-ion [32].

For $\sigma >> 0$, the value of d estimated is approximately 0.70 nm reflecting the symmetry within the ion pair (cation-anion) of the system. This thickness value found truly means that the balance between the cation-anion vs. ion-electrode interaction disposes the charge plane center at a distance of 0.70 nm from the electrode surface.

This slight increase in the value of d estimated for the anion is corroborated with the lower C(E) maximum value at more positive potentials observed in Fig. 2, reflecting the increase of thickness of the double layer. So, comparing these two systems ($[C_4MIM][Tf_2N]$ *vs.* $[C_4MIM][FAP]$) it is possible to conclude that the asymmetry of the ion pair seems not to affect the preferred orientation of the cation at the hydrophobic mercury surface. This simple approximation is also sensitive to the variation of size of the anion, since for $[FAP]^-$ anion the values of d obtained are approximately two times higher than the values estimated for $[Tf_2N]^-$ anion. Despite the simplicity of the assumptions under Eq. (3) (e.g. predicted at extremes polarizations, the EDL is essentially an Helmholtz type layer), the values extracted using this simple Helmholtz model are in agreement with the dimensions of the ions estimated by using the ChemDraw 13 software (Scheme 1).

In the case of the spheric $[FAP]^-$ anion the value of d estimated is lower than the diameter calculated from the bulk density and by assuming a cubic packing geometry (0.84 nm) [42,43]. Due to its roughly spherical shape, it is expected that changes in the orientation of the anion would not cause marked differences in the measured properties.

3.2. Au

At Au electrodes the values of differential capacity are much lower than the C(E) values obtained for Hg, Pt and GC electrodes and show a flat bell shape reasonably insensitive to the electrode potential variations. The difference in magnitude found in Hg C(E) values when compared with polycrystalline gold may rely on different imidazolium cation orientations on these two surfaces. While on Hg surface electrode it is expected that imidazolium cations interact via their alkyl side chain, on Au electrode the cation may reorient to lie flat, i.e., with the imidazolium ring interacting closely with the surface promoting the π-interactions as exemplified on Scheme 2a). The hump observed at +0.13 V *vs.* Ag may be a result of the reorientation of the $[C_4MIM]^+$ as the potential become less negative the structure would be stabilized with the anions occupying alternated positions resulting in a "checkerboard" type of structure (Scheme 2b)).The composition and the interfacial structure at Au surface appear to be reasonably insensitive to the applied potential variations suggesting that the forces that "retain" the structure are not only due to electrostatic

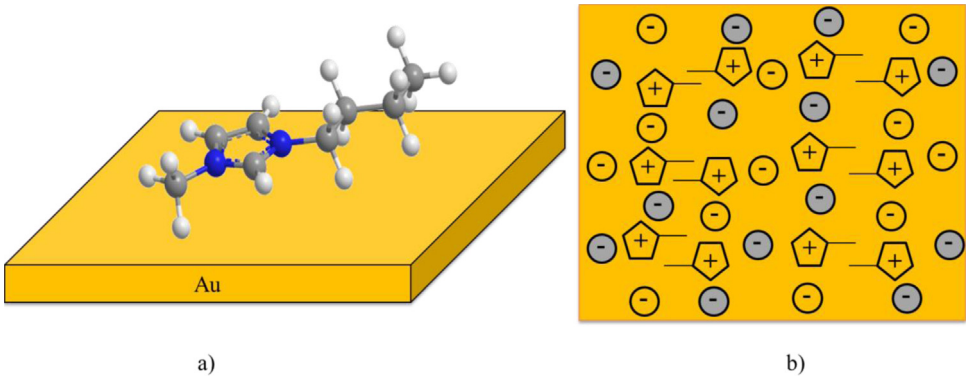

Scheme 2. a) Imidazolium cation orientation proposal at Au polycrystalline electrode. b) Representative scheme (top view) of the proposed model to describe the ions arrangement of the liquid $[C_4MIM][FAP]$ at Au interface. The non-colored ions are positioned at the electrode surface and the grey colored ions are located at the adjacent layer.

interactions with the surface [44]. This nearly constant C(E) curves within the potential interval at polycrystalline Au electrodes were also reported for the 1,5–bis(3-dimethylimidazolium) pentane di–bis(trifluoromethylsulfonyl) imide dicationic IL $[C_5(MIM)_2][Tf_2N]_2$.

Molecular dynamics simulations reveal that in the interfacial area, the polar regions of the ionic liquids are more structured than those in the bulk phase, whereas the opposite behavior was found for nonpolar regions [45]. The nearly constant C(E) curve may indicate a more compact structure than observed in the Hg electrode, since the charged imidazolium ring occupies a closer position than the alkyl hydrophobic chains at Au surface.

Recently, Hayes et al. [46] by AFM investigated the influence of the applied potential on the interfacial solvation layers in $[C_2MIM][FAP]$ and $[C_4Pyr][FAP]$ ionic liquids/Au(111) interface. The authors concluded that the charged Au(111) surface enhance the IL layering when compared to the neutral surface and they also propose a possible reorientation of cations to lay flat on the surface.

Su et al. [47] combined scanning tunneling microscopy (STM) and differential capacitance measurements to study Au(100)/$[C_4MIM][BF_4]$ surfaces. The results showed a bell-shaped C(E) with the surface reconstruction of the cation adsorption at Au single-crystal electrodes being critically dependent on the crystallographic orientation of the surfaces.

Despite having investigated Au surfaces with different topographies (polycrystalline *vs.* single-crystal surfaces), we have reproduced the C(E) curve obtained by Su et al. [47] and compared with the $[C_4MIM][PF_6]$ and $[C_4MIM][FAP]$ C(E) curve (Fig. 4).

Even though we are comparing ionic liquids containing different anionic structures and Au surfaces with different morphology it is not surprising the fact that practically the same value of capacity are obtained at more negative potentials, since the liquids are constituted by the same cation and at these potentials it is expected that the interface is essentially cation-enriched.

3.3. Pt

C(E) curve measured at polycrystalline Pt/$[C_4MIM][FAP]$ interface display distorted and asymmetric bell-shape like profile with a maximum slightly pronounced at −1.1 V *vs.* Ag ($C_{max} = 10.4 \pm 0.1\ \mu F\,cm^{-2}$). Replacing $[PF_6]^-$ by the larger $[FAP]^-$ the C(E) curves obtained show approximately two times fold increase in differential capacity values and a hump [22].

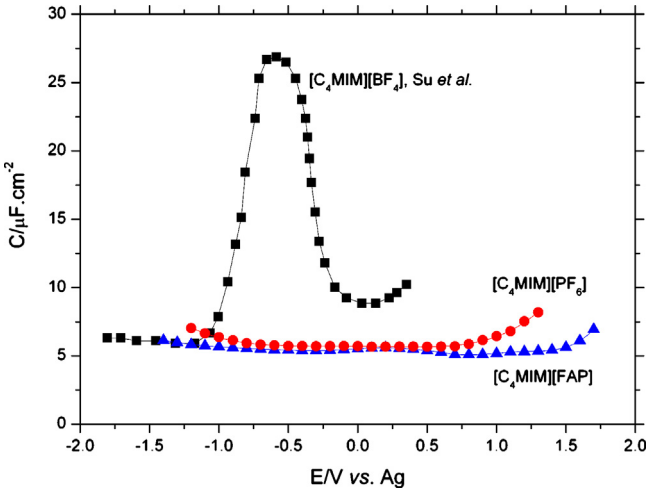

Fig. 4. Comparison of C(E) curves obtained at Au(100)/$[C_4MIM][BF_4]$ by Su et al. [47] and polycrystalline Au/$[C_4MIM][PF_6]$ and $[C_4MIM][FAP]$.

Cannes et al. [48] found that the double-layer capacitance as a function of potential to be camel shaped for Pt electrode material with the effect being more marked for the highest temperature and with a maximum observed at −0.2/−0.3 V (as reference electrode the authors used a silver wire in a 0.01 M $Ag(CF_3SO_3)$ solution in $[C_4MIM][Tf_2N]$).

Zhou et al. [49] using sum-frequency generation spectroscopic also assessed the double layer structure of neat ionic liquid (1-butyl-3-methylimidazolium trifluoromethanesulfonate ([bmim][OTf])) on Pt electrode surface. The authors demonstrated the existence of one ion layer thick. Significant adsorption/desorption hysteresis has been also reported for the anions on the Pt surface. The bell-shaped C(E) curves were also observed experimentally by Islam et al. [50] on an IL/metal electrode (platinum and gold) containing ILs with similar ion sizes.

Taking into account theoretical parameters such as the compressibility parameter γ considered in the mean-field theory proposed by Kornyshev [32] the differential capacitancy curve should be bell-shaped when $\gamma > 1/3$. The bell-shape observed on C (E) curves was also predicted by Oldham's modification [51] of the Gouy–Chapman–Stern model for ionic liquid interface in a specific case with $\gamma = 1$. However, this is still not easy to rationalize the theoretical predictions with the features observed in the experimental C(E) curves, where certainly other factors are present and have to be considered.

3.4. GC

The glassy carbon electrode/IL interface is far from being well understood. The C(E) curve obtained present U-shape with a shallow minimum ($C_{min} = 8.0 \pm 0.1\ \mu F\,cm^{-2}$). It is possible that the potential window explored on the C(E) curve at GC/$[C_4MIM][FAP]$ may not be large enough to observe the decrease in differential capacity. Since it is expected that the C(E) curve of an EDL decreases sharply when the packing of counterions reaches the steric limit, which can occur only at large electrode potentials where eventual "saturation" of the interface can occurs. Consequently, the C(E) curve begins to decrease with further increase in electrode potential. A U-shaped C(E) curve is considered to be favored on a weakly populated electrode surface [52].

Islam et al. [51] also reported U-shaped C(E) curves for [N,N-diethyl-N-methyl-N-(2-methoxyethyl) ammonium][bis(trifluoromethylsulfonyl) imide] when using GC working electrode.

Maolin et al. [52] investigated by molecular dynamics simulation how the lipophilic graphite surface affects the structure and orientation of hydrophobic $[C_4MIM][PF_6]$. The orientation calculations showed that the alkyl chains and imidazolium ring of cations both lie in the plane of the graphite surface.

Subsequently, the influence of different alkyl side chain lengths of imidazolium on the interfacial molecular structures confined between the graphite sheets were assessed using dynamics molecular simulations performed by Wang et al. [53]. The results reveal that ILs are highly compressible and present high spatial heterogeneity in the interfacial region near the graphite interface as a result of the nanosegregation which presence had already be identified in the bulk. The results also point to a preferential orientation of the imidazolium rings with the alkyl side chains on cations tend to lie flat at the graphite surface. It may be relevant to take into account that the orientation above mentioned is not conditioned by the applied potential.

Considering the EDL structure proposed to Hg electrode and taking into account the nature of the GC electrode, it is expected that the imidazolium cation probably will interact with the surface via their hydrocarbon chains. However, the distinct shape of the C(E) curves obtained in Hg and GC electrodes may point to different orientations of the ions at the interface.

Several simulation studies focused on electrode/ionic liquids interfaces evoke the role of the anisotropy of size between the ions or the charge distribution to justify the shapes of differential capacity curves [36]. However, it is difficult to discriminate the contribution of the ion-ion and ion-electrode interactions to the EDL structure.

As a result, the changes in electrode surface topography induced by electrolyte nanostructuring at the electrode/ionic liquid interface, leads to the difference in electrostatic interactions between ions, and consequently to the difference of shapes observed on C(E) curves. Different shapes of the C(E) curves for the same ionic liquid stress out the influence of the electrode-ionic liquid interactions on the preferred orientations of the ions when modeled by the applied potential.

Li et al. [54] using colloid probe atomic force microscopy (AFM) force measurements found that, for imidazolium ILs containing $[FAP]^-$, the cations located in the interfacial layer pack more closely towards the Au(111) surface at large negative potentials than the anions approach to the electrode surface at positive potentials. This method also evidenced that $[C_4MIM][FAP]$ present the weakest interfacial structure compared with shorter ethyl and longer hexyl imidazolium alkyl side chain, however, the IL interfacial nanostructure revealed to be strongly affected by the surface potential.

The results show that, despite the molecular structure of the ionic liquid is profoundly affected by the strength of dispersion interactions in the bulk, the electronic polarizability and the surface topography of the electrode dramatically influences the structure of EDL. It is comprehensible that the specific behavior of a given ion pair arrangement at electrode/ionic liquid depends upon the peculiarities of the molecular structure of the ions (ion-ion interactions) concomitantly modulated by the ion–substrate (short-range) interactions.

The roughness of the substrate is an additional parameter that should be taken into account. Vatamanu et al. [55] highlighted the importance of this parameter in shaping the C(E) curves and found that rough surface significantly affects the ion ability to reorient in order to optimize their nanostructuring at the charged surface with this effect being propagate into the first two layers.

The absence of a model that accurately predict the effect of the ion structure and chemistry of the ions present in solvent-free ILs such ionic liquids sets the challenge of a proper interpretation of the complex shape of differential capacity by changing the electrode potential.

The results showed in Fig. 2 and Fig. 3 suggest that an applicable model for ILs electrified interfaces have to take into account the chemical details of these electrolytes (ion-ion and ion-surface interactions) thus capturing the most important aspects of the EDLs obtained from experimental work. The above discussed results also suggest that the structure and composition of the interfacial ionic layer adjacent to the electrode can be adjusted by varying the applied surface potential, IL ion structure or changing the electrode material.

4. Conclusion

This works shows that EWs are affected not only by ionic liquids structure including ion shape and strong coulombic correlations between ions, but also affected by the electrode material (ion-surface interactions), highlighting the importance of the electrode material in the design of solvent properties of ILs.

The C(E) curves present distinctive shapes varying the nature of the electrode material: camel shape (Hg), flat bell shape (polycrystalline Au), asymmetric bell-shape for Pt and asymmetric U-shape for GC electrode. The minimum observed in the C(E) curve measured at Hg/$[C_4MIM][FAP]$ corresponds to the pzc (-0.45 ± 0.03 V) which was estimated from the maximum obtained in the drop time curve.

At large negative and positive potentials, the C(E) curve with higher capacity values was obtained for the GC surface probably reflecting a more efficient screening of the surface charge.

The thickness of the EDL estimated for the Hg surface using a simple Helmholtz model of 0.63 nm at $\sigma << 0$ and 0.70 for $\sigma >> 0$, are in agreement with the ion size estimated.

The role of electrode morphology and electrical characteristics of the interface cannot be neglected in the development of a model that correctly describe the structure and properties of the EDLs at the interface of ILs and electrified surfaces.

Acknowledgments

This research was carried out with financial support of FCT–CIQUP–Line 4 (PEst-C/QUI/UI0081/2013) and Renata Costa acknowledges a Pos-Doc scholarship awarded by FCT with reference SFRH/BPD/89752/2012 under the QREN – POPH – Advanced Training, subsidized by the European Union and national MEC funds.

References

[1] K. Fumino, T. Peppel, M. Rybczyńska, D. Zaitsau, J. Lehmann, S. Verevkin, M. Köckerling, R. Ludwig, The influence of hydrogen bonding on the physical properties of ionic liquids, Phys. Chem. Chem. Phys. 13 (2011) 14064.
[2] A. Fernandes, M. Rocha, M. Freire, I. Marrucho, J. Coutinho, L. Santos, Evaluation of Cation–Anion Interaction Strength in Ionic Liquids, J. Phys. Chem. B 115 (2011) 4033.
[3] X. Xuan, M. Guo, Y. Pei, Y. Zheng, Theoretical study on cation–anion interaction and vibrational spectra of 1-allyl-3-methylimidazolium-based ionic liquids, Spectrochimica Acta Part A 78 (2011) 1492.
[4] J. Lopes, A. Pádua, Nanostructural Organization in Ionic Liquids, J. Phys. Chem. B 110 (2006) 3330.
[5] K. Fruchey, C. Lawler, M. Fayer, Investigation of Nanostructure in Room Temperature Ionic Liquids using Electronic Excitation Transfer, Phys. Chem. B 116 (2012) 3054.
[6] Y. Shen, D. Kennedy, T. Greaves, A. Weerawardena, R. Mulder, N. Kirby, G. Song, C. Drummond, J. Calum, Protic ionic liquids with fluorous anions: physicochemical properties and self-assembly nanostructure, Phys. Chem. Chem. Phys. 14 (2012) 7981.
[7] T. Greaves, D. Kennedy, Y. Shen, A. Hawley, C. Drummond, Fluorous Protic Ionic Liquids Exhibit Discrete Segregated Nano-scale Solvent Domains and Form New Populations of Nanoscale Objects upon Primary Alcohol Addition, Phys. Chem. Chem. Phys. 15 (2013) 7592.
[8] G. Giffin, N. Laszczynski, S. Jeong, S. Jeremias, S. Passerini, Conformations and Vibrational Assignments of the (Fluorosulfonyl)(trifluoromethanesulfonyl) imide Anion in Ionic Liquids, J. Phys. Chem. C 117 (2013) 24206.
[9] T. Takekiyo, Y. Imai, N. Hatano, H. Abeb, Y. Yoshimura, Conformational preferences of two imidazolium-based ionic liquids at high pressures, Chem. Phys. Lett. 511 (2011) 241.
[10] Y. Wang, W. Jiang, T. Yan, G. Voth, Understanding Ionic Liquids through Atomistic and Coarse-Grained Molecular Dynamics Simulations, Acc. Chem. Res. 40 (2007) 1193.
[11] A. Triolo, O. Russina, H. Bleif, E. Cola, Nanoscale Segregation in Room Temperature Ionic Liquids, J. Phys. Chem. B 111 (2007) 4641.
[12] E. Bodo, L. Gontrani, R. Caminiti, N. Plechkova, K. Seddon, A. Triolo, Structural Properties of 1-Alkyl-3-methylimidazolium Bis{(trifluoromethyl)sulfonyl} amide Ionic Liquids: X-ray Diffraction Data and Molecular Dynamics Simulations, J. Phys. Chem. B 114 (2010) 16398.
[13] S. Kislenko, I. Samoylov, R. Amirov, Molecular dynamics simulation of the electrochemical interface between a graphite surface and the ionic liquid $[BMIM][PF_6]$, Phys. Chem. Chem. Phys. 11 (2009) 5584.
[14] A. O'Mahony, D. Silvester, L. Aldous, C. Hardacre, R. Compton, Effect of Water on the Electrochemical Window and Potential Limits of Room-Temperature Ionic Liquids, J. Chem. Eng. Data 53 (2008) 2884.
[15] C. Yao, W. Pitner, J. Anderson, Ionic Liquids Containing the Tris (pentafluoroethyl) trifluorophosphate Anion: a New Class of Highly Selective and Ultra Hydrophobic Solvents for the Extraction of Polycyclic Aromatic Hydrocarbons Using Single Drop Microextraction, Anal. Chem. 81 (2009) 5054.
[16] A. Brandt, S. Pohlmann, A. Varzi, A. Balducci, S. Passerini, Ionic liquids in supercapacitors, MRS bulletin 38 (2013) 554.
[17] M. Mezger, H. Schröder, H. Reichert, S. Schramm, J. Okasinski, S. Schöder, V. Honkimäki, M. Deutsch, B. Ocko, J. Ralston, M. Rohwerder, M. Stratmann, H. Dosch, Molecular Layering of Fluorinated Ionic Liquids at a Charged Sapphire (0001) Surface, Science 322 (2008) 424.

[18] H. Li, F. Endres, R. Atkin, Effect of alkyl chain length and anion species on the interfacial nanostructure of ionic liquids at the Au(111)–ionic liquid interface as a function of potential, Phys. Chem. Chem. Phys. 15 (2013) 14624.
[19] N. Borisenko, R. Atkin, F. Endres, Influence of Molecular Organization of Ionic Liquids on Electrochemical Properties, Electrochem. Soc. Interface 59 (2014) 59.
[20] S. Baldelli, Interfacial Structure of Room-Temperature Ionic Liquids at the Solid–Liquid Interface as Probed by Sum Frequency Generation Spectroscopy, J. Phys. Chem. Lett. 4 (2013) 244.
[21] R. Carvalhal, R. Freire, L. Kubota, Polycrystalline Gold Electrodes: A Comparative Study of Pretreatment Procedures Used for Cleaning and Thiol Self-Assembly Monolayer Formation, Electroanalysis 17 (2005) 1251.
[22] F. Silva, C. Gomes, M. Figueiredo, R. Costa, A. Martins, C. Pereira, The electrical double layer at the [BMIM][PF6] ionic liquid/electrode interface – Effect of temperature on the differential capacitance, J. Electroanal. Chem. 622 (2008) 153.
[23] A. Bard, L. Faulkner, Electrochemical Methods. Fundamentals and Applications, 2nd ed., John Wiley & Sons, Inc., 2001.
[24] F. Yang, Z. Li, S. Zhang, Q. Zhang, X. Hu, X. Zhang, Y. Deng, AC Electrochemical Stability of Ionic Liquids, Chem. Lett. 40 (2011) 1423.
[25] D. Weingarth, I. Czekaj, Z. Fei, A. Schmitz, P. Dyson, A. Wokauna, R. Kötz, Electrochemical Stability of Imidazolium Based Ionic Liquids Containing Cyano Groups in the Anion: A Cyclic Voltammetry, XPS and DFT Study, J. Electrochem. Soc. 159 (2012) H611.
[26] N. Lo, H. Chen, W. Chuang, C. Lu, P. Chen, P. Chen, Anion Reduction Dominated Cathodic Limit of Metal-Free Ionic Liquid: Experimental and Theoretical Proofs, J. Phys. Chem. B 117 (2013) 13899.
[27] D. Menshykau, I. Streeter, R. Compton, Influence of Electrode Roughness on Cyclic Voltammetry, J. Phys. Chem. C 112 (2008) 14428.
[28] V. Lockett, M. Horne, R. Sedev, T. Rodopoulos, J. Ralston, Differential Capacitance of the Double Layer at the Electrode/Ionic Liquids Interface, Phys. Chem. Chem. Phys. 12 (2010) 12499.
[29] S. Trasatti, Trends in Interfacial Electrochemistry, in: A. Silva (Ed.), D. Reidel Publishing Company, 1984.
[30] M. Alam, M. Islam, T. Okajima, T. Ohsaka, Measurements of differential capacitance in room temperature ionic liquid at mercury, glassy carbon and gold electrode interfaces, Electrochem. Comun. 9 (2007) 2370.
[31] C. Nanjundiah, S. McDevitt, V. Koch, Differential Capacitance Measurements in Solvent-Free Ionic Liquids at Hg and C Interfaces, J. Electrochem. Soc. 144 (1997) 3392.
[32] M. Fedorov, A. Kornyshev, Ionic Liquid Near a Charged Wall: Structure and Capacitance of Electrical Double Layer, J. Phys. Chem. B 112 (2008) 11868.
[33] R. Costa, C. Pereira, A. Silva, Double layer in room temperature ionic liquids: influence of temperature and ionic size on the differential capacitance and electrocapillary curves, Phys. Chem. Chem. Phys. 12 (2010) 11125.
[34] A. Kornyshev, Double-Layer in Ionic Liquids: Paradigm Change? J. Phys. Chem. B 111 (2007) 5545.
[35] M. Fedorov, N. Georgi, A. Kornyshev, Double layer in ionic liquids: The nature of the camel shape of capacitance, Electrochem. Commun. 12 (2010) 296.
[36] N. Georgi, A. Kornyshev, M. Fedorov, The anatomy of the double layer and capacitance in ionic liquids with anisotropic ions: Electrostriction vs. lattice saturation, J. Electroanal. Chem. 649 (2010) 261.
[37] M. Trulsson, J. Algotsson, J. Forsman, C. Woodward, Differential Capacitance of Room Temperature Ionic Liquids: The Role of Dispersion Forces, J. Phys. Chem. Lett. 1 (2010) 1191.
[38] Y. Lauw, M. Horne, T. Rodopoulos, F. Leermarks, Room-temperature ionic liquids: excluded volume and ion polarizability effects in the electrical double-layer structure and capacitance, Phys. Rev. Lett. 103 (2009) 117801(1).
[39] J. Vatamanu, O. Borodin, G. Smith, Molecular insights into the potential and temperature dependences of the differential capacitance of a room-temperature ionic liquid at graphite electrodes, J. Am. Chem. Soc. 132 (2010) 14825.
[40] R. Yamamoto, H. Morisaki, O. Sakata, H. Shimotani, H. Yuan, Y. Iwasa, T. Kimura, Y. Wakabayashi, External electric field dependence of the structure of the electric double layer at an ionic liquid/Au interface, Appl. Phys. Lett. 101 (2012) 053122(1).
[41] R. Costa, C. Pereira, F. Silva, Electric double layer studies at the interface of mercury–binary ionic liquid mixtures with a common anion, RSC Adv. 3 (2013) 11697.
[42] H. Li, R. Wood, F. Endres, R. Atkin, Influence of alkyl chain length and anion species on ionic liquid structure at the graphite interface as a function of applied potential, J. Phys Condens. Matter 26 (2014) 284115–284123.
[43] H. Li, F. Endres, R. Atkin, Effect of alkyl chain length and anion species on the interfacial nanostructure of ionic liquids at the Au(111)–ionic liquid interface as a function of potential, Phys. Chem. Chem. Phys. 15 (2013) 14624–14633.
[44] R. Costa, C. Pereira, A. Silva, Dicationic Ionic Liquid: Insight in the Electrical Double Layer Structure at mercury, glassy carbon and gold surfaces, Electrochim. Acta 116 (2014) 306.
[45] X. Paredes, J. Fernández, A. Pádua, P. Malfreyt, F. Malberg, B. Kirchner, A. Pensado, Bulk and Liquid–Vapor Interface of Pyrrolidinium-Based Ionic Liquids: A Molecular Simulation Study, J. Phys. Chem. B 118 (2014) 731.
[46] R. Hayes, N. Borisenko, M. Tam, P. Howlett, F. Endres, R. Atkin, Double Layer Structure of Ionic Liquids at the Au(111) Electrode Interface: An Atomic Force Microscopy Investigation, J. Phys. Chem. C 115 (2011) 6855.
[47] Y. Su, Y. Fu, J. Yan, Z. Chen, B. Mao, Double Layer of Au(100)/Ionic Liquid Interface and Its Stability in Imidazolium-Based Ionic Liquids, Angew. Chem. 48 (2009) 5148.
[48] C. Cannes, H. Cachet, C. Chouvy, C. Deslouis, J. Sanoit, C. Naour, V. Zinovyeva, Double Layer at [BuMeIm][Tf_2N] Ionic Liquid–Pt or –C Material Interfaces, J. Phys. Chem. C 117 (2013) 22915.
[49] W. Zhou, S. Inoue, T. Iwahashi, K. Kanai, K. Seki, T. Miyamae, D. Kim, Y. Katayama, Yukio Ouchi, Double layer structure and adsorption/desorption hysteresis of neat ionic liquid on Pt electrode surface — an in-situ IR-visible sum-frequency generation spectroscopic study, Electrochem. Commun. 12 (2010) 672.
[50] M. Islam, M. Alam, T. Ohsaka, Electrical Double-Layer Structure in Ionic Liquids: A Corroboration of the Theoretical Model by Experimental Results, J. Phys. Chem. C 112 (2008) 16568.
[51] K. Oldham, A Gouy–Chapman–Stern model of the double layer at a (metal)/(ionic liquid) interface, J. Electroanal. Chem. 613 (2008) 131.
[52] S. Maolin, Z. Fuchun, W. Guozhong, F. Haiping, W. Chunlei, C. Shimou, Z. Yi, H. Jun, Ordering layers of [bmim][PF_6] ionic liquid on graphite surfaces: Molecular dynamics simulation, J. Chem. Phys. 128 (2008) 134504(1).
[53] S. Wang, S. Li, Z. Cao, T. Yan, Molecular Dynamic Simulations of Ionic Liquids at Graphite Surface, J. Phys. Chem. C 114 (2010) 990.
[54] H. Li, F. Endres, R. Atkin, Effect of alkyl chain length and anion species on the interfacial nanostructure of ionic liquids at the Au(111)–ionic liquid interface as a function of potential, Phys. Chem. Chem. Phys. 15 (2013) 14624.
[55] J. Vatamanu, L. Cao, O. Borodin, D. Bedrov, G. Smith, On the Influence of Surface Topography on the Electric Double Layer Structure and Differential Capacitance of Graphite/Ionic Liquid Interfaces, J. Phys. Chem. Lett. 2 (2011) 2267.